

Active wall through a porous media foam type: flow and transfer characterization

Rafael Deptulski¹, Gisele Vieira², and Rachid Bennacer^{1,*}

¹University Paris-Saclay, LMT-ENS 94230 Cachan, France

²CEFET/RJ, DEMEC, Maracanã, Rio de Janeiro, 20271-110, Brazil

Abstract. Despite the efforts to develop new solutions to achieve the objectives of positive buildings in energy, a few studies in this area has been performed using a porous media foam type. The aim of this paper is to present the behaviour transfers of flow through a multi-structured porous media and to achieve the influence of the porosity and the thermal conductivity properties of the skeletal phase, and the interaction with a cross flow in order to get the equivalent of a perfect insulator. Therefore, in a specially made device, a finite volume method was applied to study a flow through a porous media foam-type, which was simulated to characterize the properties of the equivalent medium in terms of permeability and thermal conductivity. The analysis demonstrates that the solid phase composition and the medium porosity, as well as the distribution of pore size, are preponderant characteristics to constitute a foam structured media. Furthermore, the thermal boundary layer given by a forced convection through the porous medium has demonstrated the important influence of the flow phenomenon in a thermodynamic coupling. Lastly, three optimum configurations for the construction envisaging a balance of depleted thermal and dynamic powers for a relative conductivity $\lambda^*=10$ were found between the velocity $2 \cdot 10^{-3}$ (m/s) and $4 \cdot 10^{-3}$ (m/s).

Nomenclature

Da	Darcy number	Greek
h	convective heat transfer coefficient [W/m ² K]	μ dynamic viscosity [Pa . s]
H	pressure drop [Pa]	φ heat flux density [W/m ²]
k	permeability [m ²]	ϕ heat flux [W]
Nu	Nusselt number	ε Porosity [%]
P	pressure [Pa]	θ dimensionless temperature
Pr	Prandtl number	λ thermal conductivity [W/m.K]
Ra	Rayleigh number	Subscripts/Superscripts
Re	Reynolds number	eq equivalent value
Sc	Schmidt number	f fluid
t	dimensionless time	s solid
V	dimensionless velocity	* solid to fluid ratio

applications in several industrial and academic domains. Many research projects seek to understand the interaction behaviour between their multiple phases and predict their equivalent properties in different compositions such as metallic, polymeric or mixed foams [1,2]. Hence, several numerical methods to represent closed-cell or open-cell foam models [3,4] and theirs mechanical and hydrothermal properties have been explored [5,6].

Mancin *et al.* [7,8] analyzed the heat transfer characteristics and pressure drop for different samples of aluminum foam (5, 10, 20, 40 Pores Per Inch - PPI). They observed that the heat transfer coefficient increases with the pore density (*i.e.* the low pore size). Bhattacharya *et al.* [9] presented an analytical and experimental study to determine the equivalent thermal conductivity, permeability and inertia coefficient of highly porous metal foams. They showed that the permeability increases with the pore diameter and the porosity of the medium, but the coefficient of inertia, however, depends only on the porosity.

One of the early studies about modelling and thermos-mechanical analysis of foam-type exchangers was presented by Khaled *et al.* [10]. In order to measure the temperature profile of a heat sink and predict the overall exchange coefficient from experimental data, a three-dimensional numerical structure was modelled using a micro-tomography scan (μ-CT scan) and analyzed by a finite element method.

1 Introduction

A porous media foam type is characterized by its structure which contains a significant volume fraction of voids in addition to a continuous solid matrix that provides their structural performance. The study of transport phenomenon through porous media is increasingly researched thanks to its wide range of

* Corresponding author: rchavesd@ens-paris-saclay.fr

The adoption of different applications in porous foam type media is increasingly used thanks to its high thermal transfer capacity given by their important specific surface area and a remarkable mechanical resistance to compression. Therefore, the deal is to take advantage of this important thermomechanical potential - where the solid matrix provides mechanical support and conduct heat simultaneously; by reason of these are the two operating principles of an active wall in porous media. Hence, in further works, this system can be combined to work with several thermo-activate applications such as phase change materials [11], pre-heated air renewal or deformable porous polymers membranes [12].

Then, the main question to be answered in this research is how would be the behaviour of a flow through a foam-like porous medium coupled to a heat source (Fig.1) and how would be the development of a thermal boundary layer given by forced convection in this domain. In this study, the main investigation performed is a Finite Volume model for a non-linear heat transfer. To this extent, a porous structure based on a correlated random field is generated and its image processing is described. Thus, a mixed flow and heat transfer numerical method for Poiseuille-Rayleigh-Benard (PRB) flows to a microscopic scale is presented. Furthermore, a discussion about the results, morphological approaches, flow and heat transfer and optimum structure characterization for the thermodynamical phenomenon is carried out.

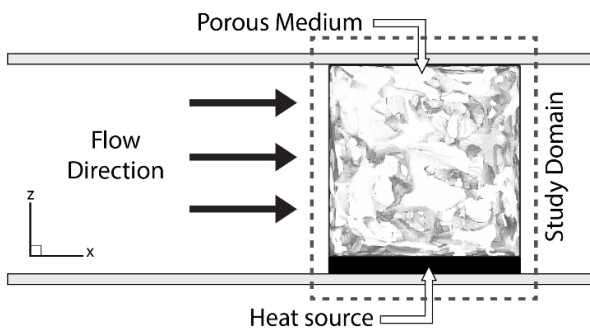


Fig.1. Porous media heat exchanger configuration.

2 Analysis and Modelling

This section covers the developing process of a three-dimensional porous medium model allocated in three steps: generating a random porous structure, controlling its morphology, as well as numerical modeling.

The random pores structure proposed was built numerically based on correlated Gaussian random fields [13], in a cube from 100 units of thickness with a triple correlation length of 10, a standard deviation of 1, expectation of 0 and 250 eigenmodes retained (Figure 2(a)). Thus, the designed structure results in a Representative Elementary Volume (REV) of a foam-like porous medium which is illustrated by the outer contour of its two phases (Figure 2(b)).

Hence, according to the construction method presented above, it is possible to change the morphology of the structure conforming to their threshold value (Figure 3 and Figure 4). Beyond this, in this work, a 90% porosity structure was chosen to be analyzed by numerical simulations (Figure 4 (c)).

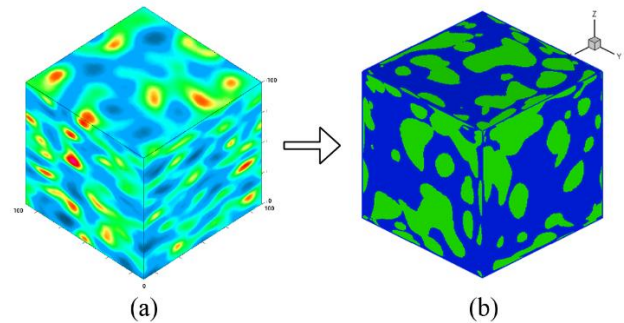


Fig. 2. Development stages to generate a porous structure based on Gaussian random draws.
 (a) Correlated Gaussian random field; (b) Image processing.

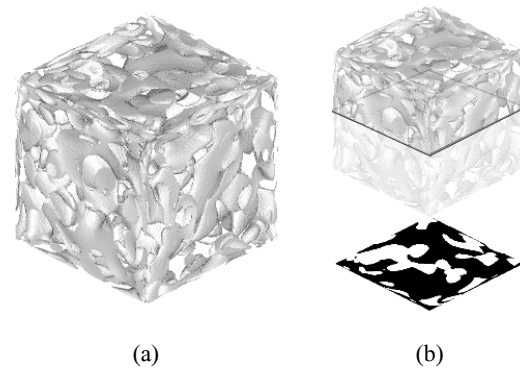


Fig. 3. (a) 3D structure; (b) phase partitioning threshold.

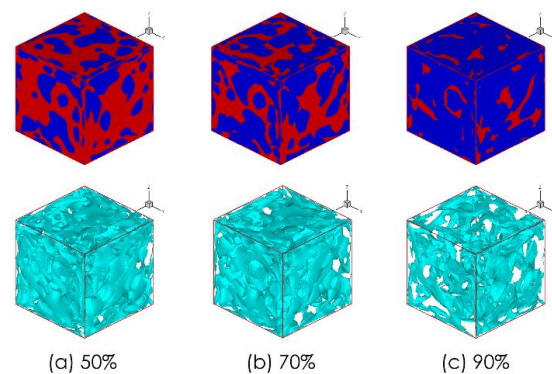


Fig. 4. Some generated structures and their external contour for 50% (a), 70% (b) and 90% (c) porosities.

In several cases, the resolution of physical problems requires a mathematical solution of complex differential equations, where the numerical resolution discretization methods can be used with the aim of solving them. In this study, a numerical device based on the Finite Volume method is implemented to study flows through porous media, it has been performed solving the energy and momentum equations. The dimensionless equations for laminar flow in three-dimensions are written

according to the following formulation, with continuity equation:

$$\nabla \cdot \vec{V} = 0 \quad (1)$$

Momentum equation:

$$\frac{\partial \vec{V}}{\partial t} + (\vec{V} \cdot \nabla) \vec{V} = -\nabla P + \frac{1}{\text{Re}} \nabla (\mu^* \nabla \vec{V}) + \frac{1}{\text{Da}} \vec{V} + \frac{\text{Ra}}{\text{PrRe}^2} (\theta + \text{NS}) \vec{k} \quad (2)$$

Energy equation:

$$\frac{\partial \theta}{\partial t} + \vec{V} \cdot \nabla \theta = \frac{1}{\text{Pr}} \nabla (\lambda^* \nabla \theta) \quad (3)$$

Additionally, the stationary flow of an incompressible fluid is governed by generalized Navier-Stokes law. For $\text{Re} \ll 1$, the equation (2) becomes:

$$\nabla P = \frac{1}{\text{Da}} \vec{V} \quad (4)$$

The continuity of both temperatures the heat flux on the solid-fluid interface is employed.

$$\theta_s = \theta_f = \frac{\partial \theta_f}{\partial n} = \lambda^* \frac{\partial \theta_s}{\partial n} \quad (5)$$

To reach a stable state solution, a convergence criterion based on the temperature field is adopted. This norm is defined by the following conditions:

$$\frac{\sum_{i,j} |\phi_{i,j}^{m+1} - \phi_{i,j}^m|}{\sum_{i,j} |\phi_{i,j}^{m+1}|} \leq \varepsilon \quad (6)$$

Where the relative error $\varepsilon = 10^{-5}$ and m is an integer that counts the number of interactions. This model has been subjected to several numerical validation tests, which have presented good accuracy conforming to reference results published in various studies [14–16].

Besides that, an experimental validation has been tested qualitatively comparing the results with those obtained by Corvaro & Paroncini [17]. Moreover, the validity of this code to the prediction of instability was verified by Bourich *et al.* [18] with good accuracy in agreement with the Hopf bifurcation test. Lastly, the calculations concerning this method have as the criterion of validity: $0,1 \leq \lambda^* \leq 200$, $\text{Ra} = 0$ and $\text{Pr} = 0,75$ with adiabatic domain boundary conditions for $\text{Re} \ll 1$ and imposed entrance boundary temperature equal to the fluid temperature before the injection for forced convection cases.

3 Results and Discussion

Heat transfer may be significantly affected by the morphology of the continuous matrix and, then, by the properties related to its porosity. Furthermore, models commonly used to assess the equivalent thermal

conductivity of a porous medium is very often based on the identification of the pore as a regular geometric structure.

Hither, we present the development of the temperature gradient in the framework after heating by the lower side (Figure 5). Moreover, some well-known approaches were collected in a state-of-the-art by Kaviany [19], modified by Bennacer *et al.* [20] and adapted in this study for the 90% porosity materials are presented in Figure 6, where can be seen also the evolution of the equivalent thermal properties of the present model.

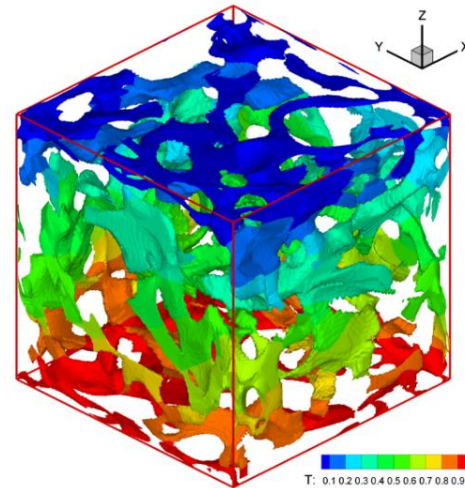


Fig.5. Temperature gradient in the porous structure.

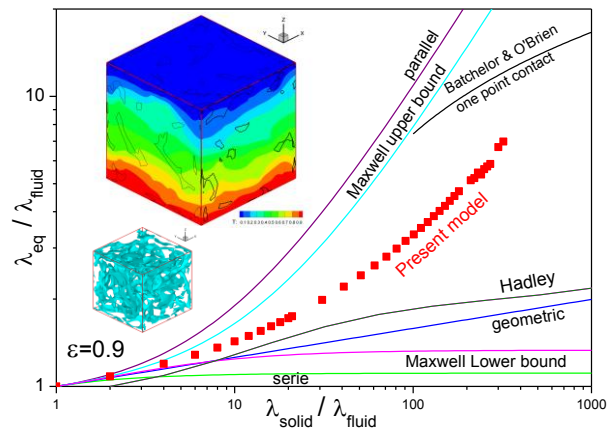


Fig.6. Ratios of thermal conductivity according to several approaches [19] [20].

In addition, among the flow resistance properties, the permeability is considered a mixed property related to the geometric characteristics of the flow medium. However, it can also be identified by certain physical properties of the transport phenomenon such as the injection velocity and the pressure drop in the flow domain. The Darcy numbers (4), shown in Figure 7, are represented by the slopes of the lines and also allows to measure the permeability of the performed medium which presents a relevant resemblance with the Kozeny-Carman model referential [21] (Figure 8).

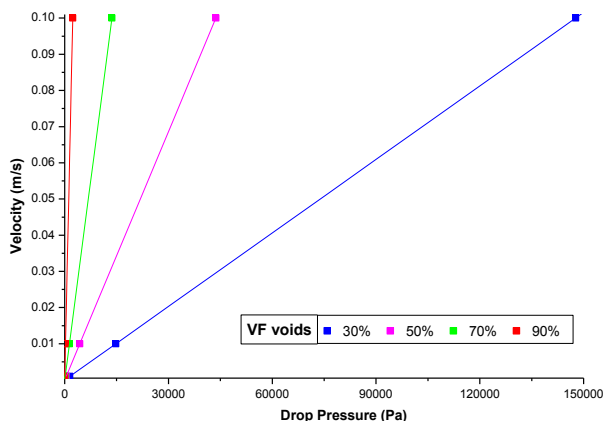


Fig.7. Numerical results for different volumetric fractions of porosity.

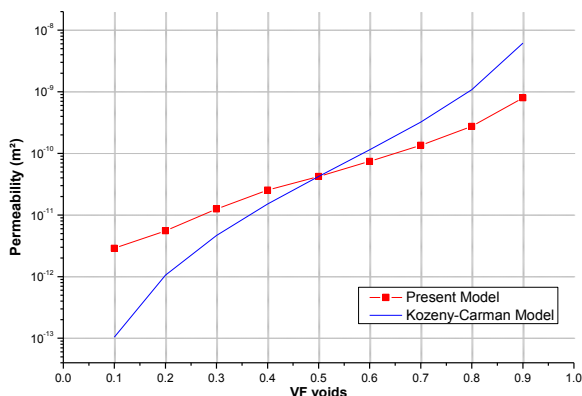


Fig.8. Material permeability in function of porosity.

Therefore, the validated Volume Finite model is used to perform the thermodynamic behaviour of the foam-type porous media, besides that, for all the analysis in this section, transient thermal and dynamic solution were considered.

Thus, three scenarios are investigated and compared having different flow injection velocity: 0, 1 and 10 (m/s) respectively (Figure 9). Firstly, the Figure 9(a) shows the temperature gradient when the system reaches steady state conduction and we observe that the temperature distribution follow the structure morphology. Then, for a low forced convection (1 m/s) in Figure 9(b), the thermal boundary layer begins to advance in the x direction. However, this development is strongly evident in Figure 9 (c) when a high forced convection (10 m/s) is applied and the thermal boundary layer is well-developed, as well as the evolution of the temperature gradient is inhibited on account of the injected flux. A remarkable feature detected it is that even with a high level of convection flux - when some validity hypothesis is technically no longer present; the numerical model continues to give the expected results in the physical sense.

Finally, to find an optimal composition for the framework, the evolution of both power requirements, injection of fluid and heating, is presented in connection

with several velocities and volume fraction of voids by a $\lambda^* = 10$.

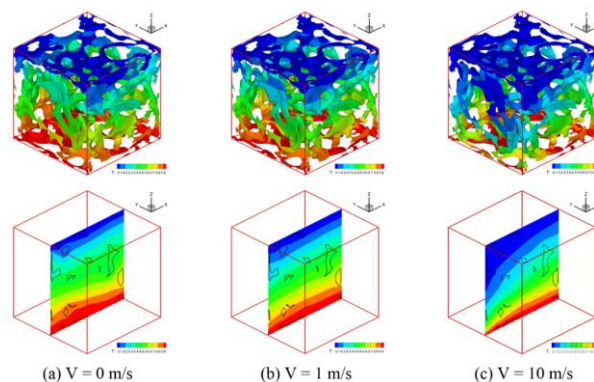


Fig.9. Evolution of thermal properties after some different convection flows: (a) a steady state of conduction; (b-c) the forced convection.

It is evident from Figure 11 that there are three velocities of injection where an optimum operating point of porosity volume fraction is found:

- (a) $V = 2 \cdot 10^{-3}$ m/s $\rightarrow \epsilon = 29\%$
- (b) $V = 3 \cdot 10^{-3}$ m/s $\rightarrow \epsilon = 48\%$
- (c) $V = 4 \cdot 10^{-3}$ m/s $\rightarrow \epsilon = 77\%$

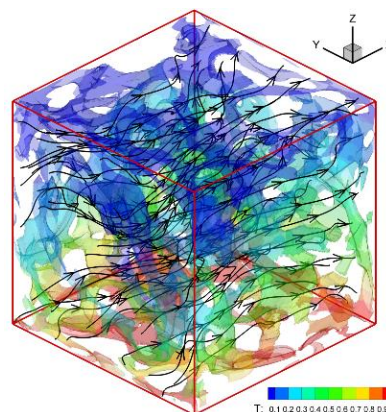


Fig.10. Flow current coupled to the temperature gradient

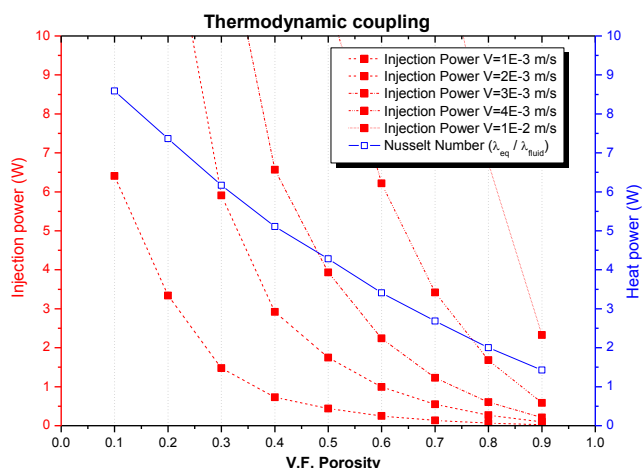


Fig.11. Optimum operating point to different velocity by $\lambda^* = 10$

4 Conclusions

This study explored the behaviour of a microscopic porous medium subjected to both imposed conditions: heat and flow. Thus, using a generation model of three-dimensional structures based on correlated random fields, a continuous solid matrix filled with non-regular pores was constructed to provide the necessary conditions to form a foam-like medium. Therefore, the characterization and optimization steps of the model were also discussed.

A numerical Finite Volume model has been performed in order to thoroughly understand the thermodynamic behaviour of foam-like porous framework and to characterize some essential properties as the thermal conductivity and the permeability in a non-linear system.

The equivalent thermal conductivity for the proposed 90% voids model increases close to the geometric middle to both homogenization boundaries models (serial and parallel). It is relevant to note that the non-uniformity of the geometry and pore distribution can result in significant variations of this type of characterization. Besides that, in the field of mass flux, the proposed model shows a significant approximation of the Kozeny-Carman model referential. Moreover, the development of the thermal boundary layer given by a forced convection through the porous medium has demonstrated the important influence of the flow phenomenon in a thermodynamic coupling. Lastly, three optimum arrangements for the construction of a porous medium envisaging a balance of depleted thermal and dynamic powers were found between the velocities $2 \cdot 10^{-3}$ m/s and $4 \cdot 10^{-3}$ m/s for a $\lambda^* = 10$ configuration.

Understanding that the coupled thermodynamic problem is a major step towards the creation of an active wall in porous media, the results presented contribute to opening up new research possibilities. These results will be helpful to further investigate the abilities of a multiphase porous media to manage their own equivalent permeability by thermoelastic polymers or to achieve an active structure to a phase change material.

Acknowledgments: We gratefully acknowledge the Laboratoire Mécanique et Technologie (LMT-Cachan) for the structure provided.

References

1. B. Jiang, C. He, N. Zhao, P. Nash, C. Shi, and Z. Wang, *Sci. Rep.*, **5**, 13825 (2015).
2. J. Zhang, N. Kikuchi, V. Li, A. Yee, and G. Nusholtz, *Int. J. Impact Eng.*, **21**, 5, 369-386 (1998).
3. Q. Fang, J. Zhang, Y. Zhang, J. Liu, and Z. Gong, *Compos. Struct.*, **124**, 409-420 (2015).
4. Z. Zheng, C. Wang, J. Yu, S. R. Reid, and J. J. Harrigan, *J. Mech. Phys. Solids*, **72**, 93-114 (2014).

5. Y. Sugimura, J. Meyer, M. Y. He, H. Bart-Smith, J. Grenstedt, and A. G. Evans, *Acta Mater.*, **45**, n°12, 5245-5259 (1997).
6. P. R. Onck, *Int. J. Mech. Sci.*, **43**, n°12, 2947-2959 (2001).
7. S. Mancin, C. Zilio, L. Rossetto, and A. Cavallini, *J. Heat Transf.*, **133**, (2011).
8. S. Mancin, C. Zilio, A. Diani, and L. Rossetto, *Exp. Therm. Fluid Sci.*, **36**, 224-232 (2012).
9. A. Bhattacharya, V. V. Calmidi, and R. L. Mahajan, *Int. J. Heat Mass Transf.*, **45**, n°5, 1017-1031 (2002).
10. K. S. Al-Athel, S. P. Aly, A. F. M. Arif, and J. Mostaghimi, *Int. J. Therm. Sci.*, **116**, 199-213 (2017).
11. [11] M. Arıcı, E. Tütüncü, M. Kan, and H. Karabay, *Int. J. Heat Mass Transf.*, **104**, 7-17 (2017).
12. C. Azra, D. Alhazov, and E. Zussman, *Polymer (Guildf)*, **58**, 162-169 (2015).
13. R. J. Adler, *The Geometry of Random Fields*. Haifa, Israel: Technion-Israel Institute of Technology, (1981).
14. A. Al Amiri, K. Khanafer, and I. Pop, *Int. J. Heat Mass Transf.*, **52**, n°15-16, 3818-3828 (2009).
15. A. Amahmid, M. Hasnaoui, M. Mamou, and P. Vasseur, *Heat Mass Transf.*, **35**, n°5, 409-421 (1999).
16. G. De Vahl Davis, *Int. J. Numer. Methods Fluids*, **3**, n°3, 249-264 (1983).
17. F. Corvaro and M. Paroncini, *Int. J. Heat Mass Transf.*, **52**, n°1-2, 355-365 (2009).
18. M. Bourich, M. Hasnaoui, M. Mamou, and A. Amahmid, *Phys. Fluids*, **16**, n°3, 551-568 (2004).
19. M. Kaviany, *Principles of Heat Transfer in Porous Media*, **53**, n°9, Springer-Verlag (1995).
20. R. Bennacer, K. Abahri, and R. Belarbi, *Sustainability of Construction Materials*. Chapter: Intrinsic properties controlling the sustainability of constructions, 2nd ed. Woodhead Publishing, (2016).
21. P. C. Carman, *Combust. Flame*, **1**, n°1, 187 (1957).